A Novel Vertical-Cavity Surface-Emitting Laser With Semiconductor/Superlattice Distributed Bragg Reflectors

Yan-Kuin Su, Jingchang Zhong, and Shoou-Jinn Chang

***Abstract*—Taking into account the tunneling effect of the superlattice, the authors present for the first time a vertical-cavity surface-emitting laser with AlAs[GaAs–AlAs] semiconductor/superlattice distributed Bragg reflectors (DBRs). The structure of a 19-period-AlAs (73.3 nm)–18.5-pair [GaAs (3.0 nm)–AlAs (0.7 nm)] DBR was grown on an n-GaAs (100) substrate by molecular beam epitaxy, and the device was fabricated by using a modified technique of proton implantation. It was found from the experiments that the peak reflectivity of the DBR is as high as 99.7%, the central wavelength is at about 840 nm, and the reflection bandwidth is wide up to 90 nm. A 20 $\times$ 20 μm^2 square mesa on the top of the DBR was made by the wet chemical etching method to measure the series resistance of the devices. It can be seen that more than a third of them are within 20–30 Ω that lead to ideal optical characteristics, low dissipated power, and reliability—some of the most important factors for the devices to be used in a number of applications in the future.**

***Index Terms*—Four-time proton implant, low series resistance, molecular beam epitaxy (MBE), semiconductor/superlattice distributed Bragg reflector (DBR), vertical-cavity surface-emitting laser (VCSEL).**

I. Introduction

VERTICAL-CAVITY surface-emitting lasers (VCSELs) have gained a lot of interest in the scientific community and in industry over the last couple of years, because their planar design and small size offer advantages in the beam characteristics, scalability, fabrication, and array configurations over their edge-emitting counterparts [1], [2]. The distributed Bragg reflectors (DBRs), which form VCSEL, determine some important optical and electrical characteristics of devices, and it is desirable to use semiconductor DBRs to allow injection current into the structure through the reflectors [3]. The required properties for DBRs are their reflectivity exceeding 99% and, simultaneously, low series electrical resistance. The high reflectivity is usually realized with a great difference in refractive indexes ($\triangle$n) and a sufficient number of quarter-wave layers. The low electrical resistance requires a sufficient doping level and a low discontinuity $\triangle$Ec in the conduction band ($\triangle$Ev in the valence band) for n-type (p-type) conduction [4]. For the short wavelength VCSELs, it is shown that the $Al_xGa_{1-x}As$–AlAs DBRs can be successfully used for both types of conduction [5]; the semiconductor DBRs lattice-matched with InP, such as InGaAsP–lnP, are designed for devices [6], [7] in the long wavelength (1.3–1.55 μm) region. Either way, the semiconductor DBRs consist only of two kinds of semiconductor materials, which we may call semiconductor/semiconductor DBRs. The semiconductor materials with large differences in refractive indexes, however, have large band-gap differences, that cause high electrical resistance and excess power consumption. Therefore, many kinds of modified heterointerface structures were designed so as to reduce the electrical resistance of semiconductor DBRs [8] which, in turn, complicate their design and fabrication and may also deteriorate the characteristics of the VCSELs.

How to compromise the problems is the key point of designing VCSEL with the desired characteristics. We replaced, in this work, GaAs in the DBR with a superlattice [GaAs–AlAs] and introduced for the first time a novel AlAs–[GaAs–AlAs] semiconductor/superlattice DBR followed by a modified proton-implant VCSEL. The tunneling effect of the superlattice with quantum size increases the tunneling current in the VCSEL that is an equivalent for decrease of the electrical resistance of the device.

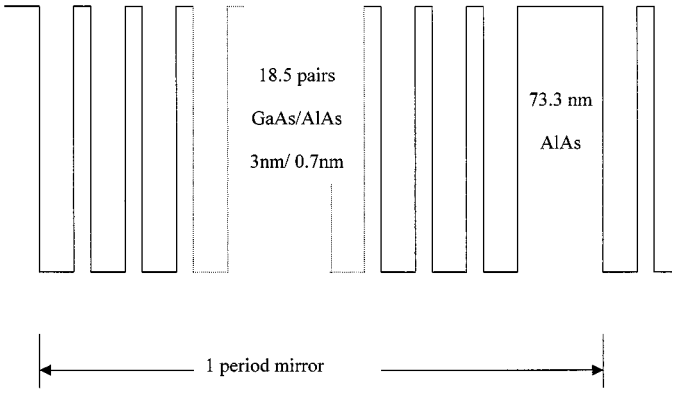

Fig. 1. The schematic diagram of the DBR structure. The AlAs (73.3 nm)/18.5-pair [GaAs (3.0 nm)–AlAs (0.7 nm)] acts as a period of the DBR.

II. DBR and VCSEL Fabrication

The structure of a 1-period AlAs–[GaAs–AlAs] superlattice Bragg mirror is shown in Fig. 1. The AlAs layer is 73.3 nm thick and the superlattice consists of 18.5-pair GaAs (3.0 nm)–AlAs

Manuscript received January 15, 2002; revised April 25, 2002.

Y.-K. Su and S.-J. Chang are with the Department of Electrical Engineering, Institute of Microelectronics, National Cheng Kung University, Tainan 701, Taiwan, R.O.C.

J. Zhong is with the Department of Electrical Engineering, Institute of Microelectronics, National Cheng Kung University, Tainan, 701, Taiwan, R.O.C. and also with the Key Laboratory of Semiconductor Lasers, Changchun Institute of Optics and Fine Mechanics, Changchun 130022, China (e-mail: zjc@public.cc.jl.cn).

Publisher Item Identifier 10.1109/LPT.2002.801086.

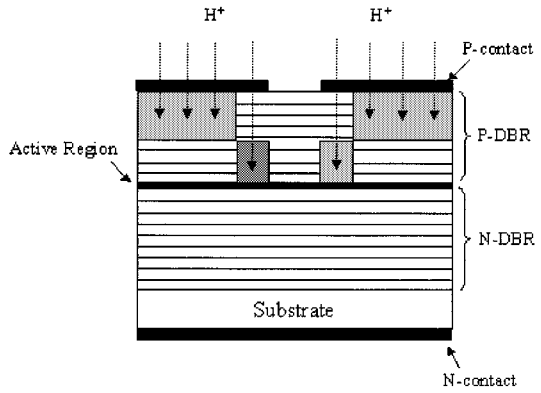

Fig. 2. The four-time implant VCSEL. The first and third bombardments with lower energy and greater dosage offered a good isolation between the devices; the second and fourth bombardments had higher energy and smaller dosage to make a good confinement for the injected current.

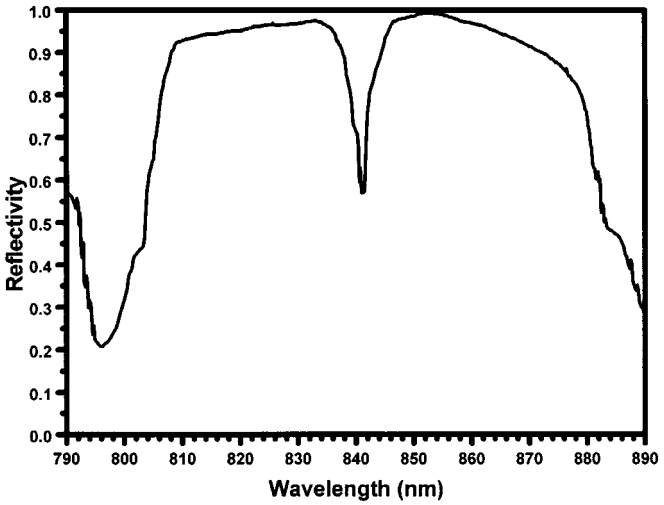

Fig. 3. The measured VCSEL reflectance spectrum. Its central wavelength is at about 840 nm. The reflection bandwidth is about 90 nm and the peak reflectivity is as high as 99.7%.

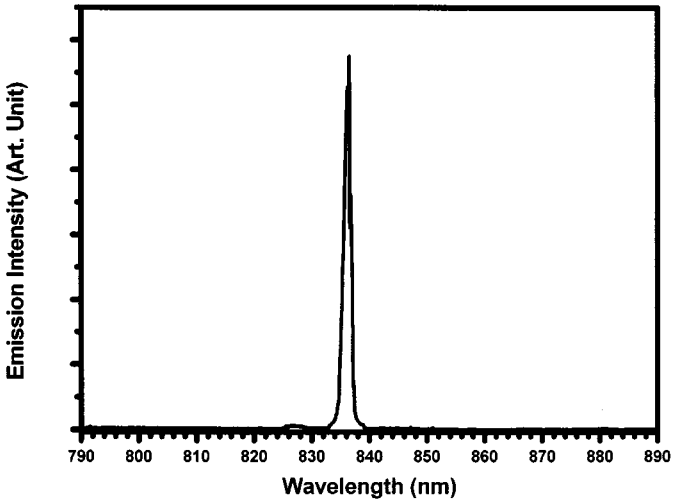

Fig. 4. The VCSEL's emission spectrum. It confirms single mode operation with the peak wavelength of about 840 nm. The spectral linewidth in this graph was limited by the spectrometer to 0.1 nm, whereas the VCSEL linewidth is actually even less than the value.

(0.7 nm). The DBR is designed for 850 nm and 19-period AlAs (73.3 nm)/18.5 [GaAs (3.0 nm)–AlAs (0.7 nm)] n-type mirrors were grown on an n-GaAs (100) substrate, following a grown 0.4-μm-thick n-GaAs buffer layer. Then, a three-quantum-well active region was routinely grown, followed by the growth of 16-period AlAs (73.3 nm)/18.5 [GaAs (3.0 nm)–AlAs (0.7 nm)] p-type mirrors. During the MBE growth, the substrate was rotated so as to ensure the epitaxial uniformity.

Besides the routine processing of the devices, there is a unique technique in this work, namely, the so-called four-time proton implant. Tungsten wires with a 20-μm diameter were taken as a mask and put closely on the epiwafer surface; then they were bombed by the protons, whose energy and dosage were 100 keV and 3.5×10^{15} cm^{-2}, respectively. The depth implanted in this case was about 1 μm and made the implanted area highly resistant electrically. Then, the wafer with the wires was evaporation coated with a 250-nm-thick Au–Zn alloy film in a vacuum system to make marks. Next, put 10-μm-diameter wires so accurately on the wafer surface that they are located on the centers of the areas shadowed by the wires in the last bombardment. The wafer was bombed again by the protons with energy of 250 KeV and dosage of 2.5×10^{15} cm^{-2}. This time, the energy higher and dosage lower than that in the first time were used to ensure the implanted depth exactly to reach to the top surface of the active region without any damage of the crystal structure. The wafer, then, was coated by a 200-nm-thick Au–Zn film in the same way as the last time. After making the wafer and wires relatively rotated 90° about each other, two more times bombardments were done in the same way as the first two times, leaving the 10×10 μm^2 square areas for current injection (see Fig. 2). The first and third bombardments with lower energy and greater dosage offered a good isolation between the devices; the second and fourth bombardments had higher energy and smaller dosage to make a good confinement for the injected current.

III. Device Characterization

The reflection spectrum of the 19-period AlAs (73.3 nm)/18.5-period [GaAs (3.0 nm)–AlAs (0.7 nm)] DBR were taken with the WDH3 model wide-wavelength scanning spectrometer (see Fig. 3), which shows that the central wavelength is at about 840 nm. The reflection bandwidth is about 90 nm and the peak reflectivity is as high as 99.7%. These parameters are suitable for the high-optical feedback needed in the VCSEL. Fig. 4 shows the VCSEL's emission spectrum, which confirms single mode operation with the peak wavelength of about 840 nm. The spectral linewidth in this graph was limited by the spectrometer to 0.1 nm, whereas the VCSEL linewidth is actually even less than the value. Using the wet chemical etching technique we made 20×20 μm^2 square mesas on top of the p-type DBR in order to measure its series resistance. The distribution of the measured resistance is shown in Fig. 5. We can see that more than a third of them are within 20–30 Ω, which are lower than that of the recent conventional DBR design with 30–40 Ω. Fig. 6 shows the LIV curves of a typical implant VCSEL device, which

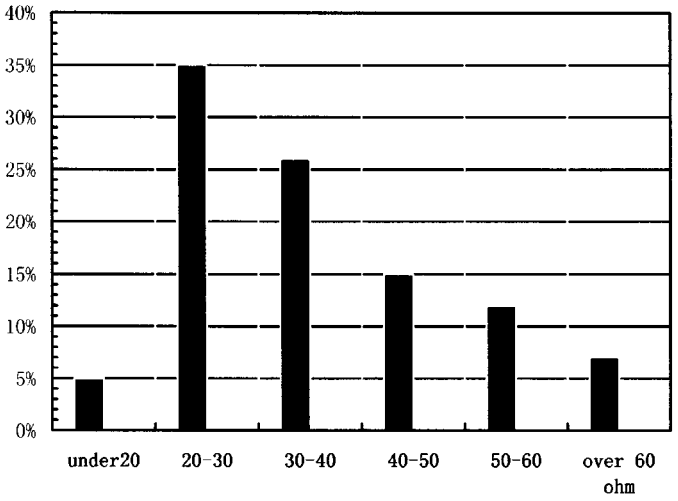

Fig. 5. The series resistance distribution of the devices. The series resistance of the devices with Bragg mirrors containing a superlattice structure shows a substantial difference compared to those achieved with conventional structures. More than a third of the measured devices have the resistance within 20–30Ω.

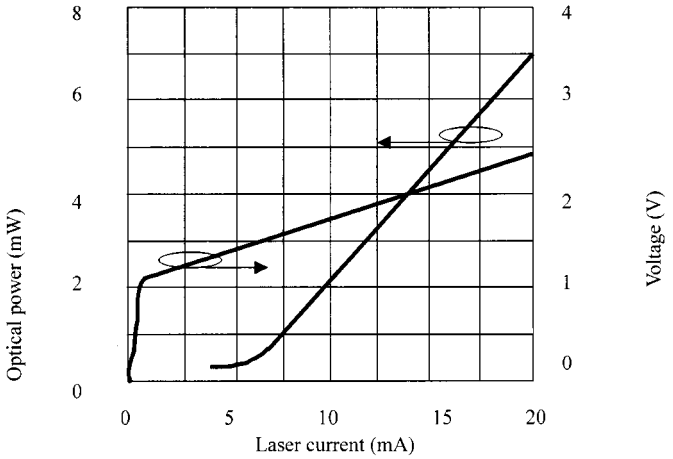

Fig. 6. The LIV curves of the implant VCSEL. The CW threshold current is about 5 mA, and the slope efficiency is between 0.35–0.45 mW/mA at room temperature.

show that the CW threshold current is about 5 mA, and the slope efficiency is between 0.35–0.45 mW/mA at room temperature.

IV. Discussion

The essential improvements for the implanted VCSEL in this work are focused on the following two points. First, we used a superlattice instead of the conventional semiconductor materials to decrease the series resistance of the VCSEL and, accordingly, the threshold and operation currents. The experiments also find it not so difficult to control the quality of the superlattice structure during the fabrication. Indeed, our first growing runs exhibited higher failure rate problems. By consequently improving the structure parameters and growth procedures, we are now able to fabricate the devices with lower failure rates that can be used to produce low cost VCSELs. Secondly, the four-time proton implant technique causes defects in the region between the active area and the bombed part that result in optical absorption. The reflection spectrum taken by the wide-wavelength scanning spectrometer shows that the optical absorption is estimated to be about twice higher than that of other techniques. Though the optical losses associated with the implanted regions affect the reliability and efficiency of the lasers (to approximately 20% for the best devices), the four-time proton implantation is worthy to be used just because of its better confinements for both beam and current, easier processing, and lower cost commercial manufacturing. The fact that the device's threshold current in CW and pulse operation slightly depends on operation temperature means that the VCSEL's characteristic temperature (T6○) is higher. It implies that the devices work stably with a long lifetime. These are the reasons that the gain guided 850-nm VCSELs using proton implantation have been widely used as light sources for various applications such as fiber optical data communication, and so on.

V. Summary

Comparing the conventional VCSEL with semiconductor/semiconductor DBRs, the new one simplifies the fabrication processing and improves the characteristics of the devices as well. The replacement of semiconductor materials with a superlattice plays a key role in this case. On the other hand, the introduction of the four-time proton implant technique into the processing technology enhances the isolation between the devices and betters the electrical confinement significantly. Both low cost and high yield of the devices are also noteworthy to be pointed out. All of these advantages make the novel VCSEL promising in the optoelectronic and other commercial applications in the coming days.

References

[1] H. Kosaka, "Smart integration and packaging of 2D VCSEL's for high-speed parallel links," *IEEE J. Select. Topics Quantum Electron.*, vol. 5, pp. 184–192, Mar.–Apr. 1999.

[2] M. S. Torre and H. F. Ranea-Sandoval, "Modulation response of multiple transverse modes in vertical-cavity surface-emitting lasers," *IEEE J. Quantum Electron.*, vol. 36, pp. 112–117, Jan. 2000.

[3] W. W. Chow, K. D. Choquette, M. H. Crawford, K. L. Lear, and G. R. Hadley, "Design, fabrication, and performance of infrared and visible vertical-cavity surface-emitting lasers," *IEEE J. Quantum Electron.*, vol. 33, pp. 1810–1824, Oct. 1997.

[4] S. F. Yu, "Analysis and design of vertical-cavity surface-emitting lasers for self-sustained pulsation operation," *IEEE J. Quantum Electron.*, vol. 34, pp. 497–505, Mar. 1998.

[5] T. E. Sale, *Vertical Cavity Surface Emitting Lasers*. New York: Wiley, 1995.

[6] I. F. L. Dias, B. Nabet, A. Kohl, J. L. Benchimol, and J. C. Harmand, "Electrical and optical characteristics of n-type-doped distributed Bragg mirrors on InP," *IEEE Photon. Technol. Lett.*, vol. 10, pp. 763–765, June 1998.

[7] F. Delorme and G. Alibert, "Reliability study of 1.55 μm distributed Bragg reflector lasers," *Electron. Lett.*, vol. 33, pp. 394–396, Feb. 1997.

[8] S. A. Chalmers, K. L. Lear, and K. P. Killeen, "Low resistance wavelength—reproducible p-type (Al, Ga)As distributed Bragg reflectors grown by molecular beam epitaxy," *Appl. Phys. Lett.*, vol. 62, no. 14, pp. 1585–1587, Apr. 1993.